

The Influence of Thermal Stress in Glass Disks on the Intensity Distribution in the Diffraction Image of a Point and on the Transfer Function

The influence of residual thermal stress in glass discs on the intensity distribution in the diffraction image of a pointobject, the resolving power and the modulation transfer function is examined.

1. Introduction

The residual thermal stresses in glass cause its birefringence, the latter, in turn, worsens the imaging quality. The question arises to what extent is this stress harmful. The first attempt to answer this question was made by KOMISSARUK [1], [2]. He assumed that the birefringence in disks is proportional to the squared distance from the disk centre. Our earlier works [3] have shown that the birefringence distribution in the thermally stressed disks is of a different type. Therefore, it is necessary to calculate the influence of the real birefringence on the imaging quality. The effect of the birefringence on the Strehl definition was estimated in [4]. The discussion in the present paper is a natural continuation of the former one.

As shown in [4] a plane wave after having passed the stressed disk suffers from splitting into two waves of deformed phase surfaces. The wave aberration of both the surfaces may be described with a formula

$$\begin{aligned} V_r(\varrho) &= V_r(1)(0.6\varrho^4 + 0.4\varrho^2), \\ V_\varphi(\varrho) &= V_\varphi(1)(0.6\varrho^4 + 0.4\varrho^2), \end{aligned} \quad (1)$$

where

ϱ — is a normalized radius in the pupil, $\varrho_{\max} = 1$.

It is more convenient to express the aberrations with the help of two other quantities i.e.

$$\begin{aligned} W(\varrho) &= \frac{1}{2}[V_r(\varrho) + V_\varphi(\varrho)], \\ R(\varrho) &= V_r(\varrho) - V_\varphi(\varrho). \end{aligned} \quad (2)$$

Both the quantities are mutually proportional

$$W(\varrho) = mR(\varrho),$$

where: m — material constant (see [3] and [4]) the typical value of which being $m = 6$.

Since the disk shifts the plane of best focus we assume

$$\begin{aligned} V_r'(\varrho) &= V_r(\varrho) + D\varrho^2, \\ V_\varphi'(\varrho) &= V_\varphi(\varrho) + D\varrho^2. \end{aligned} \quad (3)$$

Hence

$$\begin{aligned} R'(\varrho) &= R(\varrho), \\ W'(\varrho) &= W(\varrho) + D\varrho^2, \end{aligned} \quad (4)$$

where D denotes the defocusing parameter.

2. The intensity distribution

Let us assume, that a plane wave composed of elementary non-polarized waves falls onto a stressed plate located in an optical system. The time-averaged amplitude of such a wave is constant in an arbitrary direction. Denote it by a . Denote an instantaneous value of the amplitude by $A(t)$ and the components of $A(t)$ in x and y direction by $A_1(t)$ and $A_2(t)$, respectively. Consider first the component A_1 .

After passing the disk the radial and tangential components A_{1r} and $A_{1\varphi}$ of the amplitude A_1 amount to

$$\begin{aligned} A_{1r} &= A_1 \cos \varphi \exp[ikV_r(x, y)], \\ A_{1\varphi} &= A_1 \sin \varphi \exp[ikV_\varphi(x, y)], \end{aligned}$$

respectively. The exponential factors represent here the phase changes of the respective components. The projections of A_{1r} and $A_{1\varphi}$ on the axes x and y are

$$\begin{aligned} A_{1xr} &= A_{1r} \sin \varphi = A_1 \sin \varphi \cos \varphi \exp(ikV_r), \\ A_{1yr} &= A_{1r} \cos \varphi = A_1 \cos^2 \varphi \exp(ikV_r). \end{aligned}$$

Similarly, for $A_{1\varphi}$ we obtain

$$\begin{aligned} A_{1x\varphi} &= -A_{1\varphi} \cos \varphi = -A_1 \sin \varphi \cos \varphi \exp(ikV_\varphi), \\ A_{1y\varphi} &= A_{1\varphi} \sin \varphi = A_1 \sin^2 \varphi \exp(ikV_\varphi). \end{aligned}$$

*Institute of Physics of Technical University of Wrocław, Wrocław, Poland.

Hence, the components of the resulting vector in the y and x directions are:

$$\begin{aligned} A_{1x} &= A_{1xr} + A_{1xp} \\ &= A_1 \sin \varphi \cos \varphi (\exp(ikV_r) - \exp(ikV_\varphi)), \\ A_{1y} &= A_{1yr} + A_{1yp} \\ &= A_1 (\cos^2 \varphi \exp(ikV_r) + \sin^2 \varphi \exp(ikV_\varphi)). \end{aligned}$$

$$\begin{aligned} & \left| \int_{-\infty}^{\infty} \int_{-\infty}^{\infty} \sin \varphi \cos \varphi (\exp(ikV_r) - \exp(ikV_\varphi)) \exp[-2\pi i(xu + yv)] dx dy \right|^2 + \\ & + \left| \int_{-\infty}^{\infty} \int_{-\infty}^{\infty} (\cos^2 \varphi \exp(ikV_r) + \sin^2 \varphi \exp(ikV_\varphi)) \exp[-2\pi i(yx + vy)] dx dy \right|^2. \end{aligned}$$

By applying a similar procedure for the component A_2 we obtain

$$\begin{aligned} G_2(u, v) &= CA_2(t) \left\{ \left| \int_{-\infty}^{\infty} \int_{-\infty}^{\infty} \sin \varphi \cos \varphi (\exp(ikV_r) - \exp(ikV_\varphi)) \exp[-2\pi i(ux + vy)] dx dy \right|^2 + \right. \\ & \left. + \left| \int_{-\infty}^{\infty} \int_{-\infty}^{\infty} (\sin^2 \varphi \exp(ikV_r) + \cos^2 \varphi \exp(ikV_\varphi)) \exp[-2\pi i(ux + vy)] dx dy \right|^2 \right\}. \end{aligned}$$

In order to calculate the resultant intensity $G(u, v)$ the summation in $G_1(u, v)$ and $G_2(u, v)$ must be carried out together with the time-averaging. This

Since both the components A_{1x} and A_{1y} are mutually incoherent we will first calculate the propagation of the first and the second components and of the sum the intensities. Thus, the contribution to the intensity from the component A_1 , amounting to $G_1(u, v)$ will be equal to

$$G_1(u, v) = C |F\{A_{1x}\}|^2 + C |F\{A_{1y}\}|^2 = CA_1(t),$$

averaging concerns only the $A_1(t)$ and $A_2(t)$ values. Moreover, the time-averages are constants (by virtue of the assumption). Thus, we obtain

$$\begin{aligned} G(u, v) &= C \left[\left| \int_{-\infty}^{\infty} \int_{-\infty}^{\infty} (\cos^2 \varphi \exp(ikV_r) + \sin^2 \varphi \exp(ikV_\varphi)) \exp[-2\pi i(ux + vy)] dx dy \right|^2 + \right. \\ & + \left| \int_{-\infty}^{\infty} \int_{-\infty}^{\infty} (\sin^2 \varphi \exp(ikV_r) + \cos^2 \varphi \exp(ikV_\varphi)) \exp[-2\pi i(ux + vy)] dx dy \right|^2 + \\ & \left. + 2 \left| \int_{-\infty}^{\infty} \int_{-\infty}^{\infty} \sin \varphi \cos \varphi (\exp(ikV_r) - \exp(ikV_\varphi)) \exp[-2\pi i(ux + vy)] dx dy \right|^2 \right]. \end{aligned}$$

After taking account of (2) we get

$$\begin{aligned} G(u, v) &= C \left[\left| \int_{-\infty}^{\infty} \int_{-\infty}^{\infty} \cos \frac{kR}{2} \exp(ikW) \exp[-2\pi i(ux + vy)] dx dy \right|^2 + \right. \\ & + \left| \int_{-\infty}^{\infty} \int_{-\infty}^{\infty} \sin 2\varphi \sin \frac{kR}{2} \exp(ikW) \exp[-2\pi i(ux + vy)] dx dy \right|^2 + \\ & \left. + \left| \int_{-\infty}^{\infty} \int_{-\infty}^{\infty} \cos 2\varphi \sin \frac{kR}{2} \exp(ikW) \exp[-2\pi i(ux + vy)] dx dy \right|^2 \right]. \end{aligned} \quad (5)$$

Both functions R and W have a rotational symmetry and therefore we can introduce the polar coordinates

$$q = \sqrt{u^2 + v^2} \quad \text{and} \quad \Psi = \arctan \frac{u}{v}.$$

After carrying out the normalization we obtain finally

$$\begin{aligned} G(q) &= 4 \left\{ \left(\int_0^1 \varrho \cos \frac{kR(\varrho)}{2} \cos kW(\varrho) J_0(q\varrho) d\varrho \right)^2 + \left(\int_0^1 \varrho \cos \frac{kR(\varrho)}{2} \sin kW(\varrho) J_0(q\varrho) d\varrho \right)^2 + \right. \\ & \left. + \left(\int_0^1 \varrho \sin \frac{kR(\varrho)}{2} \sin kW(\varrho) J_2(q\varrho) d\varrho \right)^2 + \left(\int_0^1 \varrho \sin \frac{kR(\varrho)}{2} \cos kW(\varrho) J_2(q\varrho) d\varrho \right)^2 \right\}, \end{aligned} \quad (6)$$

where J_0 and J_2 are the Bessel functions of zero and second orders, respectively.

By putting $q = 0$ in (6) we obtain a formula for the Strehl definition, identical with that derived earlier in (3). Besides, for $R(\varrho) = W(\varrho) \equiv 0$ the formula (6) gives the intensity distribution for a perfect imaging of a point-object.

$$G(q) = \left(\frac{2J_1(q)^2}{q} \right) - \left(\frac{kR(1)}{5q} \right)^2 \{ J_1(q)[18.6428J_9(q) - 1.5000J_7(q)] - 55.4752J_5(q) - 11.0000J_3(q) - 49.3324J_1(q) - 36.0000[J_5(q) - J_1(q)]^2 + 0.0019[J_5(q) - J_3(q)]^2 \}. \quad (7)$$

In the above formula q denotes the so-called dimensionless optical coordinate

$$q = \frac{2\pi}{\lambda} r_0 \omega,$$

where r_0 — radius of the exit pupil,

ω — angular distance of the given point from the system axis measured by the angle from the entrance pupil.

The course of the function $G(q)$ was evaluated with the help of the ODR4 1204 computer. The results are presented in Fig. 1. From the graphs it may be concluded

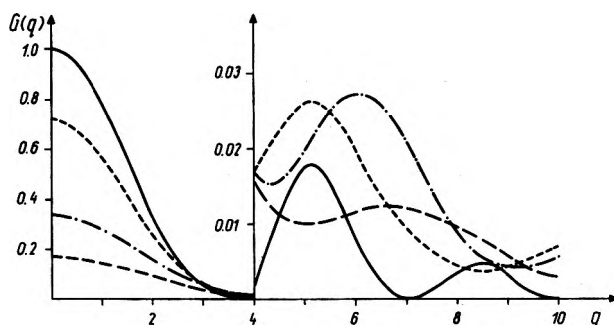


Fig. 1. The graphs of the intensity distribution in the diffraction image at the plane of best focus; $m = 6$, q is an optical coordinate

$$R(1) = \begin{array}{l} \text{—————} 0.0\lambda \\ \text{- - - - -} 0.25\lambda \\ \text{- · - · -} 0.5\lambda \\ \text{- - - - -} 1.0\lambda \end{array}$$

ded that the birefringence causes reduction in central spot intensity of the diffraction pattern (reduction in Strehl definition), while the higher order rings become brighter. Besides, the intensity at the minima does not drop to zero, as it is the case in perfect imaging ($R(1) = 0$). It is also characteristic that the central disk radius increases only slightly, consequently the two-point resolution is only slightly diminished (Fig. 2).

Now let us calculate the total amount of energy L contained in a disk of radius q .

For this reason the integral

$$L(q) = \frac{1}{2} \int_0^q q \cdot G(q) dq$$

Now, let us assume that $R(1) \leq \frac{\lambda}{4}$. Then the

integrand in (6) may be expanded into series and integrated term-after-term, whereby the terms including $R(1)$ of power greater than two may be neglected.

For example for $m = 6$ and $D = D_{opt} = -W(1)$ we obtain

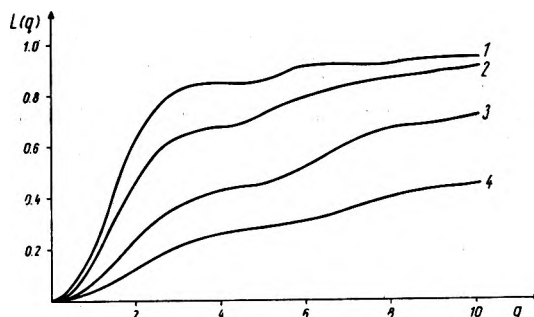


Fig. 2. A total amount of energy in the disk of radius q_0 , for the best focus plane, $m = 6$
1 — 0.0λ , 2 — 0.25λ , 3 — 0.5λ , 4 — 0.1λ

must be evaluated. The normalizing constant has been chosen so that

$$\lim_{q \rightarrow \infty} L(q) = 1.$$

In the case of perfect imaging ($R(1) = 0$) the formula transforms into the known expression

$$L_0(q) = 1 - J_0^2(q) - J_1^2(q).$$

The function $L(q_0)$ has been tabularized numerically by applying the Simpson quadrature method to the function $G(q)$, which was tabularized earlier. The results in the form of graphs are given in Fig. 2. The points of inflection correspond to the minima of $G(q)$ function (Fig. 1).

3. The two-point resolution

Let us assume that the optical system images two points as shown in Fig. 3. At an arbitrary point on the straight line passing through the centres of the images of these object points the intensity is expressed by the formula

$$G_{12}(q) = G_1(q) + G_2(q - 2q_0).$$

It is assumed, after Rayleigh, that for the self-shining sources and for ideal imaging the images are still distinguishable if the maximum of one diffraction pattern coincides with the first minimum of the other.

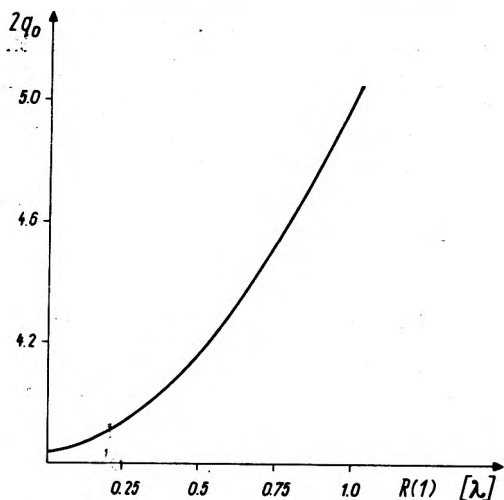


Fig. 3. The two-point resolving power versus the optical path difference at the edge of the disk, for $m = 6$

Then the intensity at the distance between the patterns drops to 0.735 of the maximum intensity value. The influence of the birefringence in the disk on the

two-point resolving power, for the incoherent light is presented in Fig. 3. The distance $2q_0$ between the diffraction spot centres, at which the intensity at the middle point between these patterns drops to 0.735 of the maximal intensity value has been accepted as a measure of the two-point resolving power. From the graph it follows that the real birefringence worsens only slightly the resolving power. It does not mean, however, that the birefringence does not deteriorate the imaging quality, as the resolving power is a poor measure of the optical imaging.

4. Optical transfer function

The transfer function for incoherent imaging is defined as a Fourier transform of the function $G(u, v)$

$$d(\tilde{x}, \tilde{y}) = F\{G(u, v)\}.$$

Let us apply the above formulae to (6). Then we obtain

$$d(s) = C \left\{ \iint_{-\infty}^{\infty} \cos \frac{kR(x, y)}{2} \cos \frac{kR(x-s, y)}{2} \exp\{ik[W(x, y) - W(x-s, y)]\} dx dy + \right. \\ \left. + \iint_{-\infty}^{\infty} \sin 2\varphi(x, y) \sin 2\varphi(x-s, y) \sin \frac{kR(x, y)}{2} \sin \frac{kR(x-s, y)}{2} \exp\{ik[W(x, y) - W(x-s, y)]\} dx dy + \right. \\ \left. + \iint_{-\infty}^{\infty} \cos 2\varphi(x, y) \cos 2\varphi(x-s, y) \sin \frac{kR(x, y)}{2} \sin \frac{kR(x-s, y)}{2} \exp\{ik[W(x, y) - W(x-s, y)]\} dx dy \right\}, \quad (8)$$

where

$$s = \sqrt{\tilde{x}^2 + \tilde{y}^2}.$$

After suitable transformations we get

$$d(s) = C \iint_{-\infty}^{\infty} \left(\sin \frac{kR(x, y)}{2} \sin \frac{kR(x-s, y)}{2} \cos 2[\varphi(x, y) - \varphi(x-s, y)] + \cos \frac{kR(x, y)}{2} \cos \frac{kR(x-s, y)}{2} \times \right. \\ \left. \times \exp\{ik[W(x, y) - W(x-s, y)]\} dx dy \right).$$

Since both the function $R(x, y)$ and $W(x, y)$ have rotational symmetry, the function $d(s)$ takes the real values. By inserting (3) and (4) into the above formula

and after some simplifications and normalizations we obtain

$$d_n(S_n) = \frac{1}{\pi} \iint_{-\infty}^{\infty} \left\{ \cos \frac{kR(1)}{2} (0.6\varrho^4 + 0.4\varrho^2) \cos \frac{kR(1)}{2} (0.6\varrho_s^2 + 0.4\varrho_s^2) + \sin \frac{kR(1)}{2} (0.6\varrho^4 + 0.4\varrho^2) \sin \frac{kR(1)}{2} \times \right. \\ \left. \times (0.6\varrho_s^4 + 0.4\varrho_s^2) \left(\frac{(s^2 - \varrho^2 - \varrho_s^2)^2}{2\varrho^2\varrho_s^2} - 1 \right) \right\} \cos[kmR(1)(0.6(\varrho^4 - \varrho_s^4) + 0.4(\varrho^2 - \varrho_s^2) + kD(\varrho^2 - \varrho_s^2))] dx dy, \quad (9)$$

where

$$\varrho^2 = x^2 + y^2,$$

$$\varrho_s^2 = (x-s_n)^2 + y^2.$$

The formula (9) was a base for numerical calculations. The results are collected in the form of graphs presented in Figs. 4 and 5. The graphs in Fig. 4 concern the optimal refocusing of the system, i.e. such a refocusing which maximizes the Strehl definition. On the

other hand, Fig. 5 presents analogical graphs for the Gaussian plane $D = 0$. A comparison of both the Figures shows that a proper focussing may considerably improve the imaging quality.

**Влияние температурных напряжений
в стеклянных дисках
на распределение интенсивности
в дифракционном изображении точки
и передаточную функцию**

Исследовано влияние остаточных температурных напряжений в стеклянных дисках на распределение интенсивности в дифракционном изображении точки, разрешающую способность и передаточную функцию контраста.

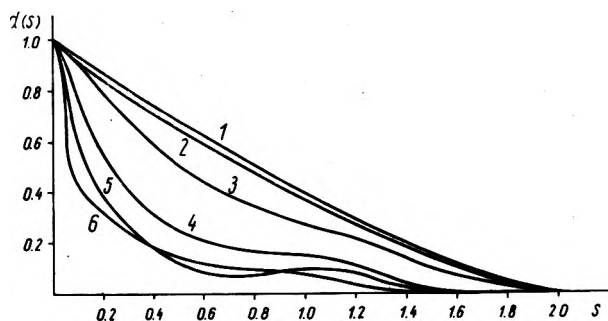


Fig. 4. Graphs of the transfer function for selected values of $R(1)$ in the best focus plane, for $m = 6$
1 - 0.0λ , 2 - 0.1λ , 3 - 0.25λ , 4 - 0.5λ , 5 - 0.75λ , 6 - 1.0λ

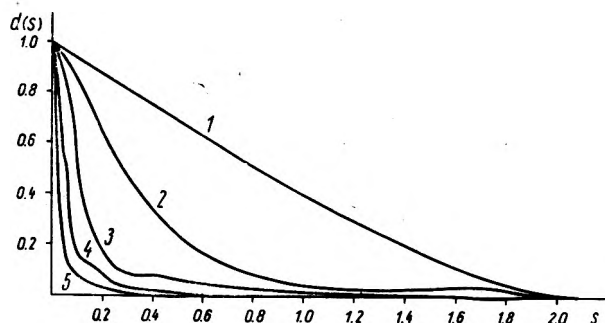


Fig. 5. Graphs of the transfer function for selected values of $R(1)$ in the Gaussian plane ($D = 0$), for $m = 6$
1 - 0.0λ , 2 - 0.1λ , 3 - 0.25λ , 4 - 0.5λ , 5 - 1.0λ

References

- [1] KOMISSARUK V. A., *Raspredeleniye osveshchennosti v izobrazhenii tochki i peredatochnaya funktsiya pri dvoynom luchepretomlenii v elementakh opticheskoy sistemy*, Opt. Spekr. 31, 1, 178-182 (1970).
- [2] KOMISSARUK V. A., BELAYEV A. G., *Raspredeleniye osveshchennosti v izobrazhenii tochki pri dvoynom luchepretomlenii v opticheskoy systemie*, Opt. i Spekr. 32, 4, 825-826 (1972).
- [3] RATAJCZYK F., LISOWSKA B., PIETRASZKIEWICZ K., *Changes of the refractive index in the thermally stresses glass disks*, Optica Applicata 4, 3, 41-44 (1974).
- [4] PIETRASZKIEWICZ K., RATAJCZYK F., *Influence of thermal stresses existing in glass disks on the Strehl definition*, Optica Applicata 4, 4, 7-10 (1974).

Received December 19, 1975